

Contents lists available at ScienceDirect

Solar Energy

journal homepage: www.elsevier.com/locate/solener





A photothermal solar tunnel via multiple transparent $Fe_3O_4@Cu_{2-x}S$ thin films for heating utility application

Anudeep Katepalli ^a, Yuxin Wang ^a, Jou Lin ^a, Anton Harfmann ^b, Mathias Bonmarin ^c, John Krupczak ^d, Donglu Shi ^{a,*}

- ^a Materials Science and Engineering Program, Department of Mechanical and Materials Engineering, College of Engineering and Applied Science, University of Cincinnati, Cincinnati. OH 45221. USA
- ^b College of Design, Architecture, Art and Planning, University of Cincinnati, Cincinnati, OH 45221, USA
- ^c School of Engineering, Zurich University of Applied Sciences, 8400 Winterthur, Switzerland
- d Department of Engineering, Hope College, Holland, MI 49423, USA

ARTICLE INFO

Keywords: 3D solar harvesting Spectral selective films Energy-neutral Photothermal energy generation Transparent multi-panels

ABSTRACT

A Photothermal Solar Tunnel Radiator (PSTR) is designed and developed by employing multiple transparent photothermal glass panels (TPGP). The primary objective is to pioneer a transformative approach to achieve energy-neutral building heating utilities, exemplified by a lab-scale "Photothermal Solar Box" (PSB) exclusively heated with TPGP under natural sunlight. The PSTR presents a novel paradigm for sustainable energy, enabling direct solar energy capture through transparent glass substrates with photothermal coatings. The high transparency of Fe₃O₄@Cu_{2-x}S coated glass substrates enhance efficient solar harvesting and photothermal energy generation within the Photothermal Solar Box. The system demonstrates an impressive thermal energy output, reaching up to 9.1 \times 10⁵ joules with 8 photothermal panels in parallel. Even under colder conditions (ambient temperature: 8 °C), with accelerated heat loss, the interior temperatures of the PSB without any thermal insulation achieve a commendable 40 °C, showcasing effective photothermal heating in cold weather. These findings indicate the system's resilience and efficiency in harnessing solar energy under diverse conditions, including partial cloudy weather. The initiative contributes to broader sustainability goals by providing a scalable and practical alternative to traditional solar heating methods, aligning with the global mission for a cleaner, greener future

1. Introduction

In the pursuit of achieving a net-zero future by 2050, as declared at COP26, the development of an advanced living system that is energy-neutral, zero-emission, and climate-positive becomes imperative. With residential and commercial buildings accounting for a substantial portion of total energy consumption, a transition to energy-neutral structures could lead to substantial benefits, including reduced utility costs, enhanced grid reliability, improved air quality, public health, and a carbon-free environment [1]. Addressing the pressing energy challenges, solar energy utilization stands out as a key approach with numerous technical, environmental, and ecological advantages [2,3]. While photovoltaic (PV) solar cells have been widely adopted for various

applications, their implementation poses several challenges [3–10], leading to a call for innovative and more efficient alternatives.

Despite the apparent abundance of solar energy in nature, the processes involved in solar harvesting and energy conversion using traditional PV systems can be costly and environmentally impactful. 2D PV systems rely on flat surfaces for solar harvesting, limiting the area exposed to sunlight. This constraint becomes particularly problematic in densely populated areas where available land is scarce. The inefficiency of utilizing only 2D surfaces hinders the potential for maximizing solar energy absorption, especially when aiming for enhanced energy density [11]. The extensive land use required for traditional 2D PV installations presents challenges, especially when considering the scarcity of available land in urban environments. As urbanization continues to rise,

Abbreviations: PSTR, Photothermal Solar Tunnel Radiator; PV, Photovoltaic; PT, Photothermal; PSB, Photothermal Solar Box; TPGP, Transparent Photothermal Glass Panels; AVT, Average Visible Transmittance; LPD, Light Power Density.

E-mail address: shid@ucmail.uc.edu (D. Shi).

^{*} Corresponding author.

finding suitable spaces for solar farms or large-scale PV installations becomes increasingly challenging. This limitation impedes the scalability of 2D PV systems for widespread energy production.

The utilization of solar energy for building utility heating purposes has traditionally relied on photovoltaic (PV) solar systems. Solar building utility heating systems comprise several key components designed to harness and utilize solar energy for heating applications. At the core of these systems are solar collectors, which can be either photovoltaic panels converting sunlight into electricity or solar thermal collectors absorbing sunlight to generate heat [9,10]. A crucial element is the heat transfer fluid, such as water, glycol, or synthetic heat transfer fluids, responsible for conveying heat from the collectors to storage or heating systems. The heat exchanger facilitates the transfer of heat from the fluid to the building's heating system, while a storage tank stores heated fluid for later use, ensuring a continuous energy supply during periods of low sunlight. A control system monitors and optimizes system operation, and a distribution system transports heated fluid to various heating points within the building. Complementary components include a back-up heating system for periods of low solar availability, insulation to minimize heat loss, and, in some cases, integration with existing heating infrastructure. These components work synergistically to maximize the efficiency of solar building utility heating systems.

While solar building utility heating systems offer sustainable and renewable energy solutions, these systems often entail high initial installation costs, and their space requirements, especially in densely populated areas, may be substantial. Storage limitations, seasonal variations affecting efficiency, and the need for regular system maintenance further contribute to the complexity of solar heating adoption. Integrating these systems with existing heating infrastructure can be intricate, and some individuals may find solar collectors aesthetically unappealing. Technological advancements and evolving policies are continuously addressing these challenges, aiming to enhance efficiency, cost-effectiveness, and widespread adoption of solar building utility heating systems.

In response to these challenges, there is a growing recognition of the need for three-dimensional solar harvesting solutions [12–17]. Innovations in this direction aim to overcome the limitations of traditional 2D PV systems, offering more efficient, sustainable, and scalable alternatives for solar energy utilization. For building utility heating purposes, it can be more efficient to directly convert solar light to thermal energy via photothermal heating. Recognizing that high energy density requires a large surface area, a novel transparent multilayer system was developed for solar light harvesting in three-dimensional space [12–15]. This innovative concept, illustrated in Fig. 1a, employs transparent

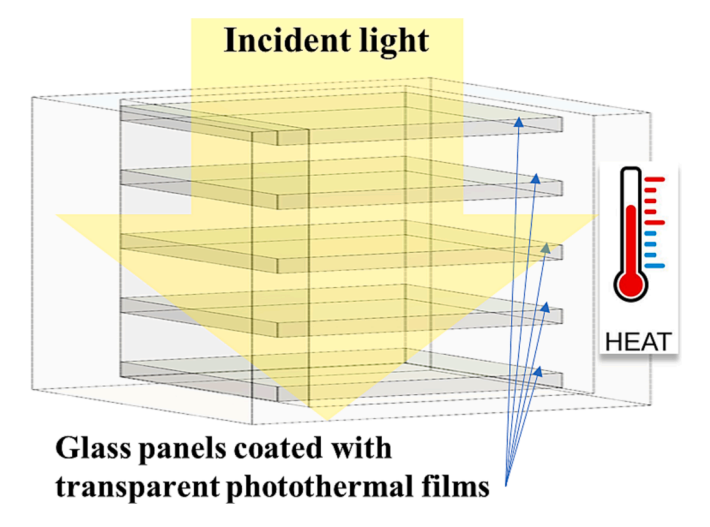


Fig. 1. Schematical diagram showing 3D solar harvesting and energy generation via multiple transparent photothermal thin films.

photothermal (PT) thin films that allow solar light to penetrate multiple panels, activating the photothermal heating on each layer. This approach significantly enhances energy density and solar harvesting efficiency. Through multi-panels in a confined volume, the PT films efficiently collect photons, offering a promising avenue for advancing solar harvesting technology for building utility heating. This research seeks to address the shortcomings of traditional PV utility heating systems by proposing a more economic and efficient solar harvesting solution with transparent PT thin films.

Based on the multiple transparent PT panels as shown in Fig. 1, in this study, a novel concept is developed known as Photothermal Solar Tunnel Radiator (PSTR), presenting a paradigm shift in solar harvesting methodologies. Central to this innovative system is the utilization of multiple transparent panels with photothermal nano coatings, as depicted in Fig. 2. The PSTR envisions a transformative approach to energy sustainability by directly harvesting solar energy through an array of transparent glass substrates, each coated with a photothermal film containing plasmonic Fe₃O₄ nanoparticles (Fig. 2). Fig. 2 illustrates the core components of this novel system, showcasing a solar tunnel, acting as a solar – activated radiator. The solar tunnel's dome captures sunlight, channeling it through the transparent glass substrates adorned with photothermal coatings. Upon exposure to solar irradiation, these coatings efficiently convert photons into heat, elevating the surface temperature of the substrates. Functioning as a thermal radiator, the heated substrates radiate the captured solar energy without the need for external power sources or additional forms of energy. This direct solar harvesting mechanism represents a significant advancement in harnessing natural sunlight for energy-neutral systems, marking a departure from traditional energy-intensive approaches. It should be noted that a diffuser is placed at the end of the PSTR as a lighting source for a room space where sunlight does not directly reach.

One promising avenue in advancing solar energy applications is the direct conversion of solar light to thermal energy via photothermal heating, which comes with several notable advantages over conventional PV solar heating methods. Photothermal heating stands out for its simplicity and cost-effectiveness, potentially eliminating the need for heat transfer fluid, heat exchanger, storage tank in some applications. This streamlined approach results in lower installation and maintenance costs, making it an economically attractive option for building utility heating. Furthermore, the efficient energy conversion achieved through photothermal heating, bypassing multiple stages present in traditional PV utility heating systems, minimizes energy losses, and optimizes overall energy utilization. Innovations in three-dimensional solar harvesting, exemplified by the transparent multi-panel system, address the limitations of 2D PV systems, providing a larger surface area exposed to sunlight and significantly enhancing energy density for building utility heating. The scalability and sustainability advantages of photothermal heating, particularly in three-dimensional solar harvesting, contribute to its appeal, offering a simple, eco-friendly, and scalable solution aligned with environmental goals.

The primary objective of this research is to pioneer a transformative approach towards achieving energy-neutral building heating utilities, as exemplified in Fig. 2. To materialize this vision, a lab-scale "solar house" is developed that can be heated exclusively with multi-panel photothermal thin films under natural sunlight. This innovative initiative seeks to address the pressing challenges associated with traditional building heating methods, which often rely on conventional energy sources, contributing to environmental degradation and increased energy consumption. By leveraging the unique properties of multilayer photothermal thin films, our research endeavors to create a sustainable and energy-efficient solution for building heating utilities. The envisioned "solar house" will serve as a tangible representation of our commitment to harnessing solar energy directly for heating purposes, reducing dependence on non-renewable energy sources, and mitigating the environmental impact associated with conventional heating systems.

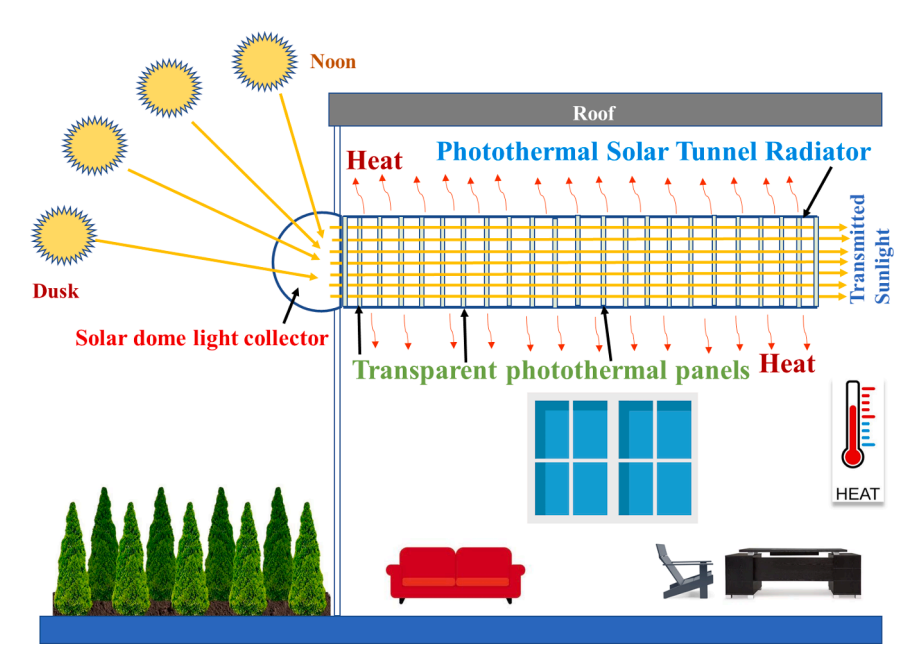


Fig. 2. Schematic diagram showing the concept of Photothermal Solar Tunnel Radiator (PSTR).

In essence, this research serves as a crucial step and alternative approach towards realizing energy-neutral building heating utilities by directly converting the solar light to thermal energy for enhanced efficiency. Through the development and evaluation of the lab-scale "photothermal solar house," we aspire to pave the way for scalable and practical applications of multilayer photothermal thin films in the realm of building heating, offering a more sustainable and eco-friendlier alternative to traditional heating methods.

2. Experimental procedure

2.1. Synthesis of Fe3O4@Cu2-xS nanoparticles and deposition of thin films

Following the established literature for the synthesis process of $Fe_3O_4@Cu_{2\cdot x}S$ nanoparticles [12–18], a 60 ml oleylamine solution was heated to 300 °C in a nitrogen environment, and $Fe(acac)_3$ in oleylamine/N-methyl-2-pyrrolidone was injected. The resulting solution was maintained at 300 °C until well mixed, then cooled to 60 °C. Fe_3O_4 nanoparticles were collected, washed with methanol, and dried by freeze drying. $Cu_{2-x}S$ coating involved heating a specific amount of Fe_3O_4 nanoparticle solution to 70 °C. A mixture of sulfur in oleylamine/cyclohexane was injected, followed by a mixture of $Cu(acac)_2$ in oleylamine/chloroform, forming $Fe_3O_4@Cu_{2\cdot x}S$ nanoparticles collected, washed, and dried.

For thin film deposition, 10 ml of $Fe_3O_4@Cu_{2\cdot x}S$ nanoparticle solution was mixed with 80 ml of epoxy resin. The polymer solution was stirred for 5 min, ensuring even mixing and removal of trapped air bubbles. 10ml of this solution was evenly distributed on each of eight glass panels resulting in $Fe_3O_4@Cu_{2\cdot x}S$ concentration of 0.006 mg/cm² on each panel, achieving 75% AVT. Panels cured overnight and are ready for use once the polymer solution is fully cured.

2.2. Design of a "Photothermal solar Box"

For developing a lab-scale "Photothermal Solar Box" (PSB), larger photothermal glass panels were coated with the Fe_3O_4 @Cu_{2-x}S thin films. To simulate the building conditions, a PSB is designed as shown in Fig. 4. As shown in this figure, a vertical solar tunnel is constructed within a transparent PMMA box with dimensions of 50 cm (length) \times 37

cm (width) \times 50 cm (height). This tunnel accommodates eight removable transparent photothermal glass panels (TPGP) arranged in a vertical stack. To enhance solar energy utilization, the interior of the tunnel is covered with mirrors. Each TPGP has dimensions of 18 cm (length) \times 13 cm (width) \times 3 mm (height). The experiments are designed to explore the heating effectiveness of the tunnel under diverse weather conditions and various experimental setups.

To simulate the sunlight and environmental conditions, two types of configurations of PSB are designed: (1) the PSB is uncovered therefore exposing TPGP to the incoming sunlight at various incoming angles (Fig. 3a), (2) PSB covered with white Styrofoam packing sheet for two purposes (Fig. 3b): (a) simulate a window by harvesting sunlight only through the opening area, (2) reflect the sunlight to avoid the surface

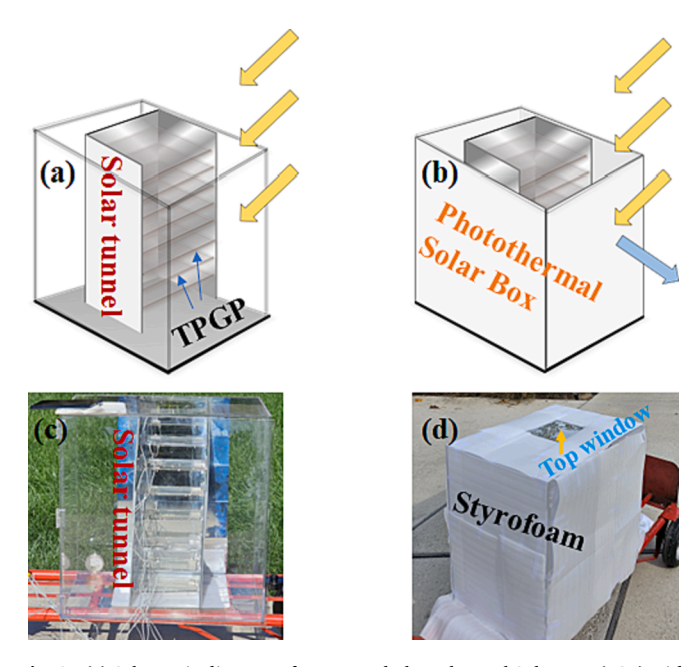


Fig. 3. (a) Schematic diagram of uncovered Photothermal Solar Box (PSB) with exposed Transparent Photothermal Glass Panel (TPGP); (b) schematic of PSB covered with Styrofoam; (c) photograph of the uncovered PSB; and (d) photograph of the covered PSB with Styrofoam.

heating. Fig. 3c and d are photographs of the uncovered and covered PSB, respectively. As shown in these configurations, solar light can be harvested in different ways depending on the time of the day and season. Based on the concepts depicted in Figs. 1 and 2, the photothermal effect can be activated on each TPGP for generation of heat, raising the interior temperature. The goal of this experiment is to determine the sufficient thermal energy generated via TPGP that is capable of maintaining a comfortable room temperature in cold climate (\sim 0 °C).

2.3. Temperature monitoring

For monitoring temperatures, K-type thermocouple thermometers were employed to track the temperatures of both the photothermal panels and the PSB. Additionally, an FLIR camera was utilized to capture infrared images, providing valuable insights into the thermal distribution of the system.

The average visible transmittance (AVT) of the photothermal panels is controlled at 75%, while that of the PMMA box is 93%. The experiments were consistently initiated at 2 PM on the main campus of University of Cincinnati under all recorded weather conditions. Light power density (LPD) during experiments varies, with a maximum of 0.048 W/cm² on sunny days and a minimum of 0.0001 W/cm². LPD was measured using a Newport optical power meter model 1600-R.

The transparent PSB is strategically covered with Styrofoam on all sides, leaving a square cut on the top side to allow light to pass through. This design choice is integral to certain experimental conditions, facilitating a comparative analysis with an uncovered PSB. This comparison aims to assess the influence of light intensity and angle on the photothermal heating capacities of the system.

During winter and rainy scenarios, the PSB is insulated to systematically analyze the rate of heat loss from the system to the external environment. It's noteworthy that the experimental setup concerning light angle dependence is intentionally not oriented with the angle of the sun. This deliberate choice allows for an examination of the impact of shadows on the photothermal panels, providing comprehensive insights into the system's performance under various conditions.

2.4. Time dependence of solar light incident angle for photothermal measurements

Fig. 4 shows the experimental spatial configuration, measurement times, and corresponding solar angles. The photothermal experiment consistently initiated at 2 PM on a given day in the month of October and November 2023, and the corresponding solar angle is indicated in Fig. 4a and b. The entire experiment began at 2 PM and ended at 6 PM while the solar angle changed from 11° to 73°. Due to the solar angle variation, the light power density (LPD) is also changing as shown in Fig. 4c. As can be seen in this figure, LPD linearly decreases from 48 mW/cm² to 30 mW/cm² between 2 PM and 5 PM. LPD decreases more

rapidly between 5 PM and 6 PM. As shown in this figure, the PSB is positioned with the top "window" facing up and four vertical walls directed in all directions as indicated.

3. Results

3.1. Characterization of the Fe3O4@Cu2-xS nanoparticles and thin films

The synthesis and characterization of Fe₃O₄@Cu_{2-x}S nanoparticles and thin films have been previously reported [18-23]. The characterization results of the transparent Fe₃O₄@Cu_{2-x}S thin films are shown in Fig. 5. Fig. 5a shows the transmission electron microscopy (TEM) image of the Fe₃O₄@Cu_{2-x}S nanoparticles. As can be seen in this figure, the nanoparticles are monodispersed with an average diameter of 15 nm. Upon deposition of the nanoparticle solution on glass substrate via spin coating, uniform thin films were obtained [22]. Fig. 5b shows the changes in temperature increase, ΔT , as a function of time for the Fe₃O₄@Cu_{2-v}S thin films of various concentrations irradiated by simulated solar light with power of 0.1 W/cm². The temperature increase at the beginning is rather rapid due to the photothermal effect of the thin films, however reaching a plateau after about 5 min. This plateau is formed as a result of heat loss through the environment so that the temperature increase can no longer be sustained by photothermal heating. The light is turned off at 10 min and temperature is thereafter decreasing rapidly for all concentrations. As shown in Fig. 5b, the heating curves are consistent with the film concentrations that the highest ΔT reaches 7 °C for Fe₃O₄@Cu_{2-x}S at the concentration of 5.08 \times 10^{-4} g/cm^2 .

The optical absorption of the $Fe_3O_4@Cu_{2-x}S$ thin film is shown in Fig. 5c. With a strong absorption in the UV region, the Fe₃O₄@Cu_{2-x}S thin film shows a minimum around 600 nm and a broad absorption extending into the NIR range peaking at 1200 nm (Fig. 5c). [22] This unique optical feature of the Fe₃O₄@Cu_{2-x}S film provides the strong absorptions in UV and NIR for thermal energy conversion and high transmittance in the visible range for multilayer designs. For comparison, the optical absorption of the Fe₃O₄ thin film is also shown in Fig. 5c. As can be seen in this figure, the Fe₃O₄ thin film exhibits strong UV absorption, but no peak observed in the near-infrared (NIR) region. This "U"- shaped characteristic absorption spectrum as shown in Fig. 5c was obtained by an addition of Cu_{2-x}S in the Fe₃O₄ system, creating a typical core-shell structure which is responsible for the broad and large NIR absorption [12]. Previous studies have shown that the strong NIR absorption of the Fe₃O₄@Cu_{2-x}S film is responsible for enhanced photothermal effect [22].

As a result of the optical characteristics shown in Fig. 5c, the $Fe_3O_4@Cu_{2-x}S$ film appears quite transparent. Fig. 5d shows the photograph of a $Fe_3O_4@Cu_{2-x}S$ film in front of a building on the campus of University of Cincinnati. As can be seen from the photograph, consistent with the "U" – shaped optical characteristic shown in Fig. 5c,

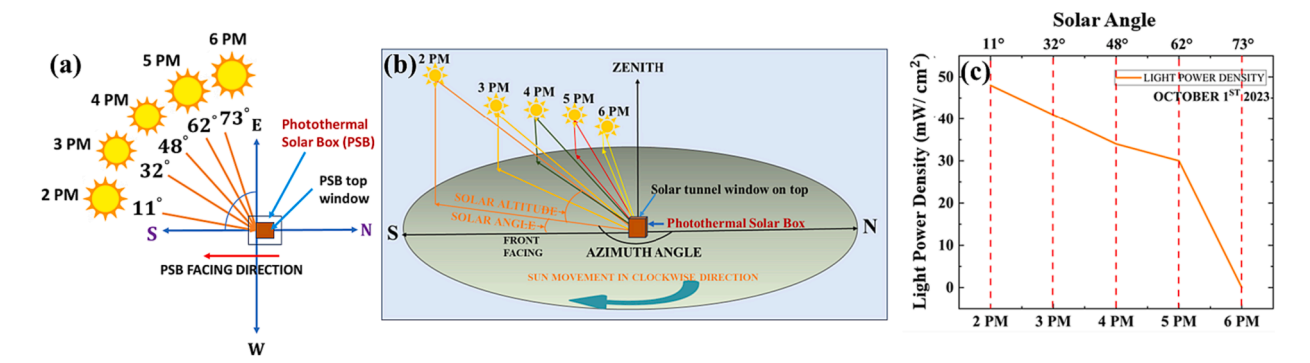


Fig. 4. (a) Variation in solar angle over time in relation to the orientation of the Photothermal Solar Box (PSB); (b) three-dimensional depiction showing the spatial alignment of solar angles throughout time, correlated with the orientation of the PSB; and (c) time and solar angle dependence of light power density.

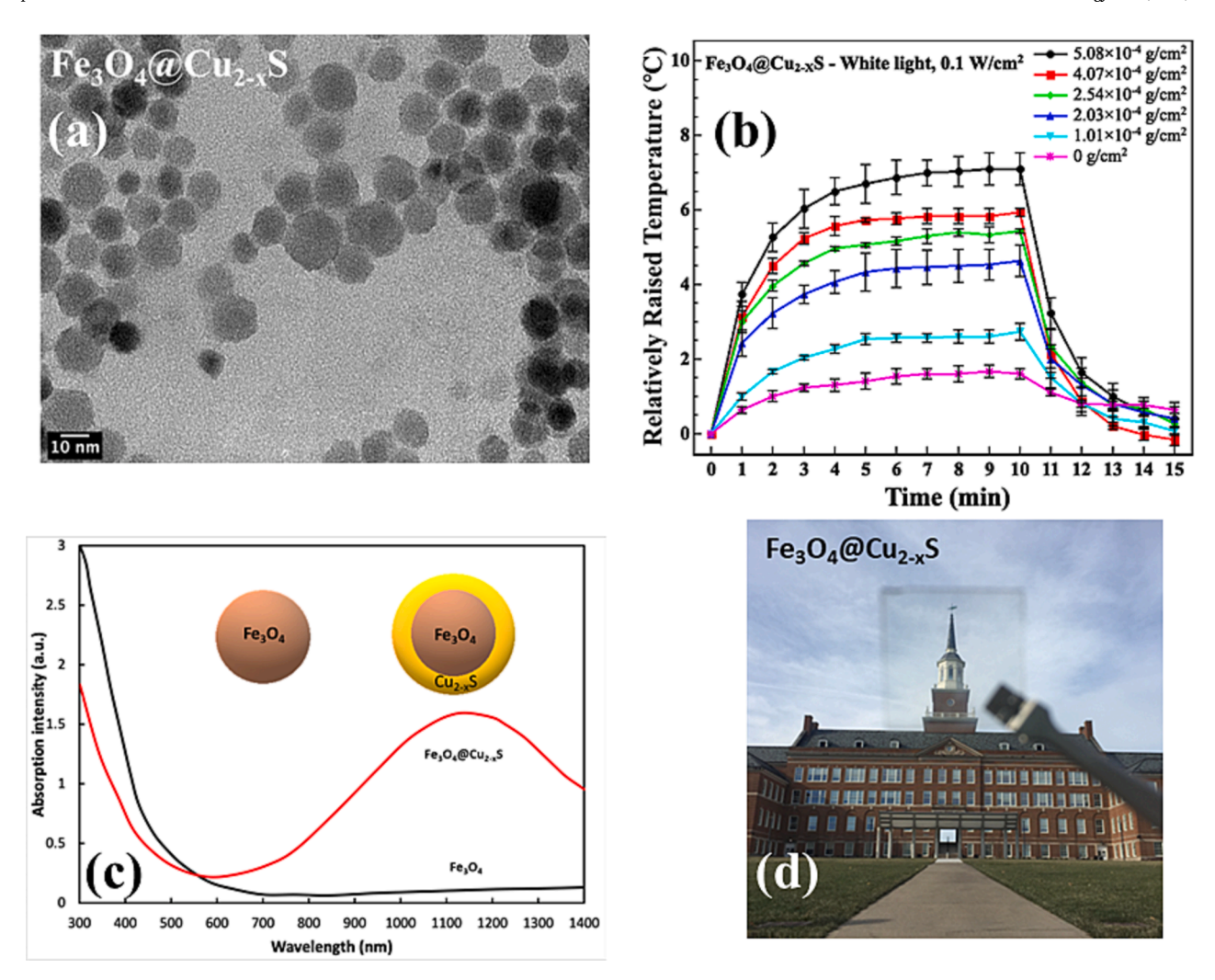


Fig. 5. (a) TEM image $Fe_3O_4@Cu_{2,x}S$ nanoparticles; (b) heating curves of $Fe_3O_4@Cu_{2,x}S$ thin films with different nanoparticle concentrations indicated; (c) optical absorption of the $Fe_3O_4@Cu_{2,x}S$ thin film; (d) photograph of the $Fe_3O_4@Cu_{2,x}S$ thin film.

the film is highly transparent resulting in a clear image of the building in a distance. High light transmittance in the "optical window" is one of the fundamental characteristics and requirements of PSTR, enabling solar light harvesting through multiple panels in a confined 3D space.

3.2. Light power density

Fig. 6a shows the optical photograph of a single layer transparent photothermal glass panel (TPGP). As can be seen in this figure, the TPGP is quite transparent with AVT of 75%. The UV–Vis spectrum of the TPGP is shown in Fig. 6b, exhibiting the typical "U" – shaped characteristic, responsible for the high AVT value. These TPGP are arranged in parallel as shown in Fig. 6c with a total of 8 panels. The light power density (LPD) was measure on October 2nd, 2023, on the main campus of University of Cincinnati under partially sunny/cloudy weather (see Fig. 6a). As shown in Fig. 6d, LPD consistently decreases from 50 to 6 mW/cm² as the number of TPGP increases from 1 to 8.

3.3. Photothermal experiments

The photothermal experiments using the Photothermal Solar Box (PSB) was conducted on October 2nd, 2023, on the main campus of University of Cincinnati with all the conditions detailed in Fig. 5. The solar intensity of the day ranged between 0.048 W/cm² and 0.030 W/cm². Fig. 7a shows the schematic PSB that is uncovered allowing solar

light to fully shine on the transparent photothermal panels to generate thermal energy. The heating curves are shown in Fig. 7b. As can be seen in this figure, the temperatures of all 8 TPGP experience rapid increase initially and level off forming plateaus until the sunlight is blocked at 150 min. As pointed by the arrows as shown in Fig. 7a, the incoming sunlight is at an angle as illustrated in Fig. 5. Note that the experiment started at 2 PM so the initial angle is at 11°. Therefore, each TPGP registers photons of varied intensity, resulting in different temperatures. Interestingly, as shown in Fig. 7b, the middle TPGP exhibits the highest temperature around 65 °C (layer 4, green), while the top one (layer 8, brown) has the lowest temperature 54 °C. As shown in Fig. 4, due to solar angle variation, the light power density changes with time. Correlating the solar angle change to the Solar Tunnel configuration in Fig. 3a, it is found that the middle layers in fact experience more solar exposures, while uncovered. Additionally, with the highly reflective mirrors inside the solar tunnel, these middle layers provide more photothermal heating compared to top and bottom layers. Two different LPD values are indicated in Fig. 7b: 0.048 mW/cm² at 3 PM and 0.035 mW/cm² at 4 PM. As shown in Fig. 7c, the infrared images show the temperature distributions of the PSB under the natural sunlight. As can be seen in this figure, the PSB is heated up quite uniformly due to the photothermal effect of the films.

Thermal energy is defined as $Q=\Delta T_{max}\times m\times Cp$, where ΔT is the maximum temperature difference raised by a given number of thin films, m is the mass of the sample (thin film + substrate), and Cp is the specific

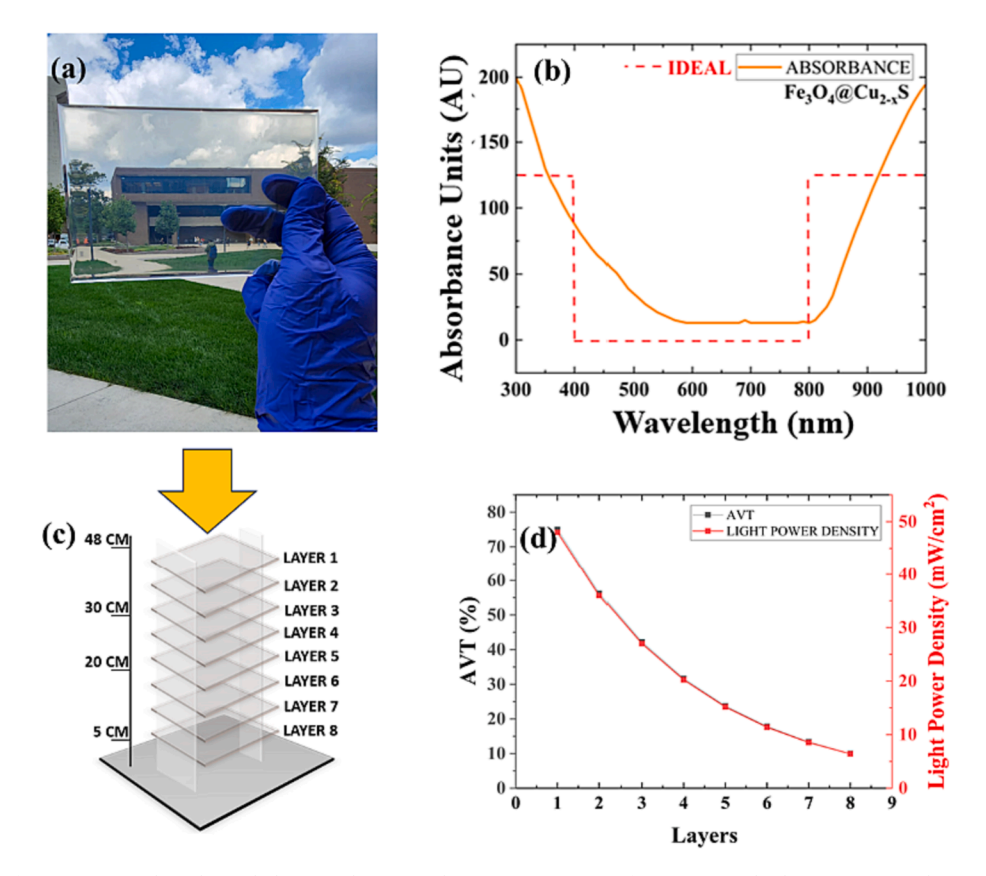


Fig. 6. (a) Photograph of a transparent photothermal glass panel (TPGP); (b) UV–Vis spectrum of TPGP; (c) Multiple TPGP arranged in parallel in the solar tunnel; and (d) light power density as a function of number of TPGP.

heat of glass panel (the PT films are extremely thin). The thermal energy is calculated based on the heating curves of the Fe₃O₄@Cu_{2-x}S films installed in the PSB and plotted against the number of layers as shown in Fig. 7c. Fig. 7d illustrates the increase in heat energy generation as adding more TPGP (e.g., 1, 1+2, 1+2+3...). The thermal energy calculation exclusively considers the heating curve, omitting the cooling curve, as its purpose is to portray the maximum heat energy generation across different layer stacks. As shown in this figure, the thermal energy generated is consistent with the heating curves shown in Fig. 7b. For a single panel in the PSB, the system generates about $1.3\times10^5~\mathrm{J}$ thermal energy. As more panels are added, the thermal energy generated is consistently increasing up to $1.13\times10^6~\mathrm{J}$ for a total of 8 panels.

A numerical simulation of the thermal energy balance was conducted to verify the heat transfer modes in the photothermal solar box. The finite difference method was utilized. At any given time, the rate of temperature change of nodes inside the box depends on the heat capacity of the element and the difference between heat generation (for photothermal materials) and heat transfer by conduction or convection from the element. The primary mode of heat loss from the box was modeled as heat transfer by conduction through the walls of box and convective heat transfer between the outer box surface and ambient air. The ambient air far from the box was assumed to be isothermal at 25 $^{\circ}$ C. The dimensions and parameters described in the experimental procedure were used. For the photothermal substrates and PMMA box a heat capacity of 1.0 kJ/(kg·K) and thermal conductivity of 0.15 W/(m·K) were used. The system of equations describing the element thermal energy balance were solved numerically using the SciPy Odeint module from the Python scientific computing library. Numerical simulation results are summarized by a plot of average internal photothermal box temperature as a function of time. The temperature calculated by numerical simulation for the test is in reasonable agreement with the measured temperatures. Fig. 7e shows the agreement between the

numerical simulation of the energy balance provides confidence of a general consistency between simulated and actual heat transfer modes in the photothermal solar box.

Fig. 8a shows the optical photograph of the PSB that is covered with white Styrofoam packing sheet allowing solar light to only enter the PSB through the top window. The heating curves are shown in Fig. 8b. As can be seen in this figure, the temperatures of all 8 TPGP experience rapid increase initially and level off forming plateaus until the sunlight is blocked at 135 min. However, since the PSB is covered, the limited solar light results in considerably lower heating temperature with the highest at 51 °C. Under this condition, the solar light can only enter the PSB from the top window. Consistently, the top panel (panel 1 black) is heated to the highest temperature, while the bottom one (panel 8 brown) has the lowest temperature of 42 °C. Note that the experiment also started at 2 PM with the initial solar angle at 11°. Even with the system covered, the PSB is uniformly heated as shown in the thermal image (Fig. 8c). Fig. 8d shows the thermal energy generated by the number of TPGP. As can be seen in this figure, even with the PSB covered, the system can still generate maximum thermal energy up to 9.1×10⁵ J, which is comparable to that of the uncovered PSG.

To simulate cold climate, the photothermal experiments were carried out on November 2nd, 2023, with the atmosphere temperature of 8 °C. The purpose of the experiment was to determine the capability of TPGP in raising the interior temperature in cold environments. As shown in Fig. 9a, the weather is sunny with LPD between 0.048 W/ cm² and 0.030 W/ cm². The time of the experiment started at 2 PM. The temperature monitoring is shown in Fig. 10b. For temperatures within the solar tunnel, the thermometers are placed between the first and second panels, third and fourth panels, fifth and sixth panels, and seventh and eighth panel panels. For PSB interior temperatures, the thermometers are place at different heights (5, 20, 30, 48 cm) outside the solar tunnel as shown in Fig. 10b.

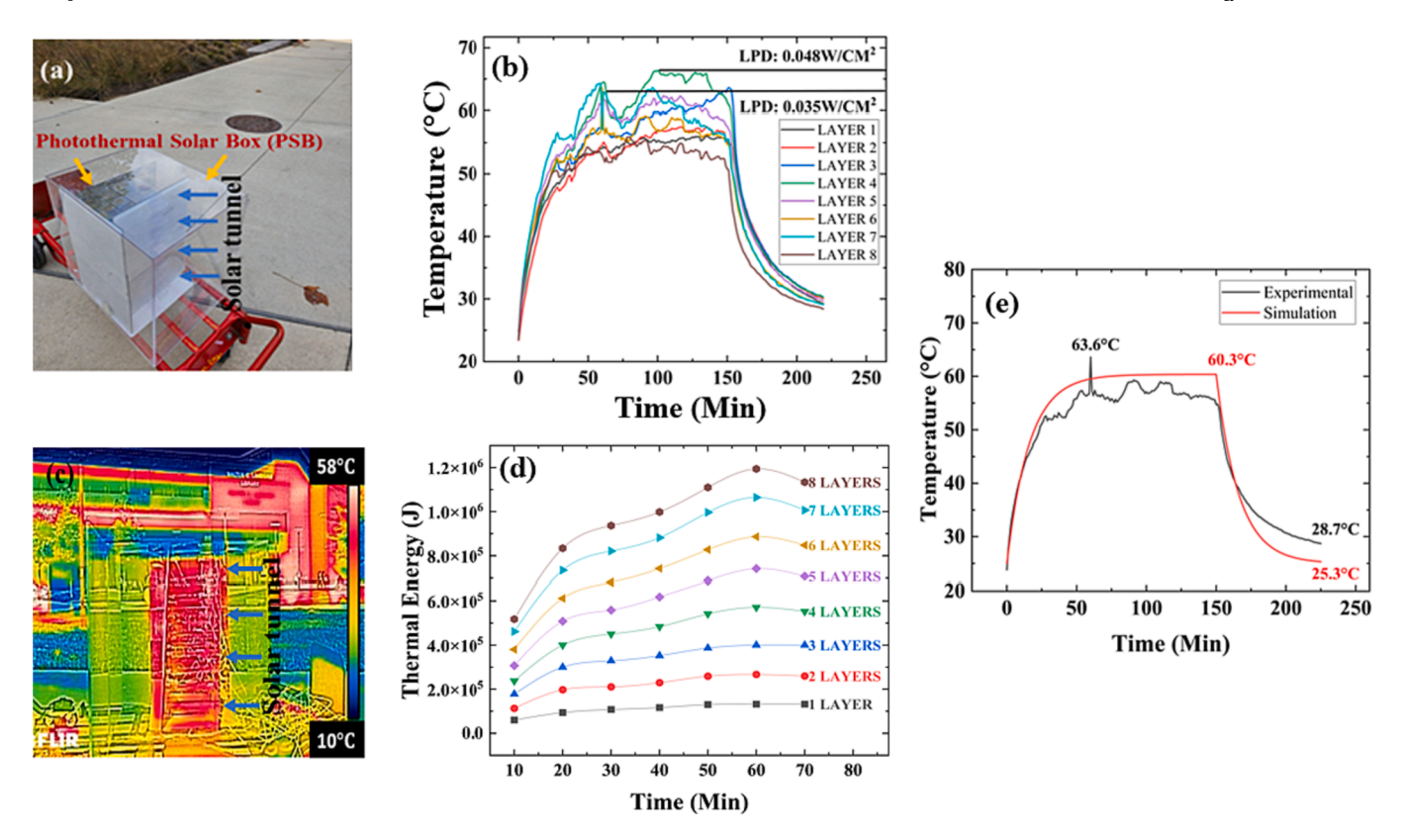


Fig. 7. (a) Schematic diagram showing the uncovered Photothermal Solar Box (PSB); (b) heating curves of different Transparent Photothermal Glass Panels (TPGP); (c) infrared thermal image of the PSB with 8 panels of Fe₃O₄@Cu_{2-x}S films (75 % AVT) under natural sunlight; (d) thermal energy vs number of panels; and (e) comparison of heating curves for PSB under experimental and simulated conditions. The experiment was carried out on October 2nd, 2023, on the main campus of University of Cincinnati at 2 PM. Sunny weather. Light power density: 0.048 W/cm² and 0.030 W/cm². Ambient temperature: 25 °C.

Fig. 9c shows the heating curves of the TPGP. Quite different from those taken in October with higher ambient temperature of 25 °C (Figs. 7 and 8), the temperatures increase less rapidly and reach maximums at 70 min for all panels. No temperature plateaus are sustained due to rapid heat loss. As can be seen in this figure, the temperature of the bottom panels has increased to 50 °C. More remarkably, as shown in Fig. 9d, the interior temperatures of the PSB can reach 40 °C at 5 cm and 30 cm indicating sufficient photothermal heating in cold weather (8 °C).

Fig. 10a shows the photothermal experiments with an uncovered PSB under the same condition (ambient temperature 8 $^{\circ}$ C). Due to exposure to more solar light, as shown in Fig. 10b, the TPGP temperature can reach even above 60 $^{\circ}$ C at the top panel. More impressively, the interior temperatures of the PSB can reach 55 $^{\circ}$ C at 5 cm and 50 $^{\circ}$ C at 30 cm indicating sufficient photothermal heating in cold weather (8 $^{\circ}$ C).

A recent experiment was conducted on January 20th, 2024, during the winter season in Cincinnati, Ohio, with the primary objective of assessing photothermal heating power at low ambient temperatures (-10 °C). In Fig. 11a, a snapshot of the outdoor photothermal experiments features a partially insulated PSB. The insulation involves three side walls covered with Styrofoam, leaving one side wall, the top, and the bottom uncovered for enhanced exposure to sunlight. Fig. 11b provides an illustration of the thermometer placements both inside and outside the solar tunnel, while Fig. 11c presents the heating curves of the TPGP with thermometers positioned between the photothermal panels. Notably, the TPGP temperature reaches 40°C at layers 3-4 despite an outdoor temperature of merely $-10\,^{\circ}$ C. The lower plateau in the curves is attributed to moving clouds leading to reduced Light Power Density (LPD). Remarkably, the interior temperatures of the PSB can reach 35°C at a depth of 30 cm, indicating effective photothermal heating power even in extreme cold weather (-10°C) . Fig. 11c and 11d highlight a rapid decline in temperatures within 20 min after sunlight obstruction at 80 min, with even more accelerated cooling (RC) observed at 100 min, indicating substantial temperature differentials between the interior of the PSB and the external environment.

The Photon Conversion Efficiency (PCE) $\boldsymbol{\eta}$ is calculated with the equation below [24]:

$$\eta = \frac{\left(C_g m_g + C_{PTmaterial} m_{PTmaterial} + C_{polymer} m_{polymer}\right) \Delta T_{\text{max}}}{IA \Delta t}$$

$$\approx \frac{C_g m_g \Delta T_{max}}{IA \Delta t} \times 100\%$$
(1)

where g is glass, c is the specific heat capacity (J/g. $^{\circ}$ C), m is mass (g), ΔT max is the maximum change in temperature increase in the sample (°C), I is the incident light power density (W/cm²), A is the surface area of the sample, and Δt is the time required for a sample to reach the maximum temperature (s) [24]. Fig. 12 shows the Photon Conversion Efficiency (PCE) of the Photothermal Solar Box (PSB). Without cover, the solar tunnel captures photons from both the top and front sides (Fig. 3a), ensuring favorable Light Power Densities (LPD) across all Photothermal Glass Panels (PTGP). The top panel attains a 34% PCE, and when all 8 layers are combined, there's a remarkable 321% increase in net PCE compared to a single layer due to consistent light attenuation. When the PSB is covered, the solar tunnel receives photons only from the top side (Fig. 3b), resulting in a reduced PCE of a single layer to 28.5%. However, the use of mirrored surfaces in the solar tunnel leads to a collective 198% PCE improvement across all 8 layers compared to a single layer. The mirrored solar tunnel proves crucial, directing photons to the bottom layers and enhancing the overall PCE of the PSB significantly.

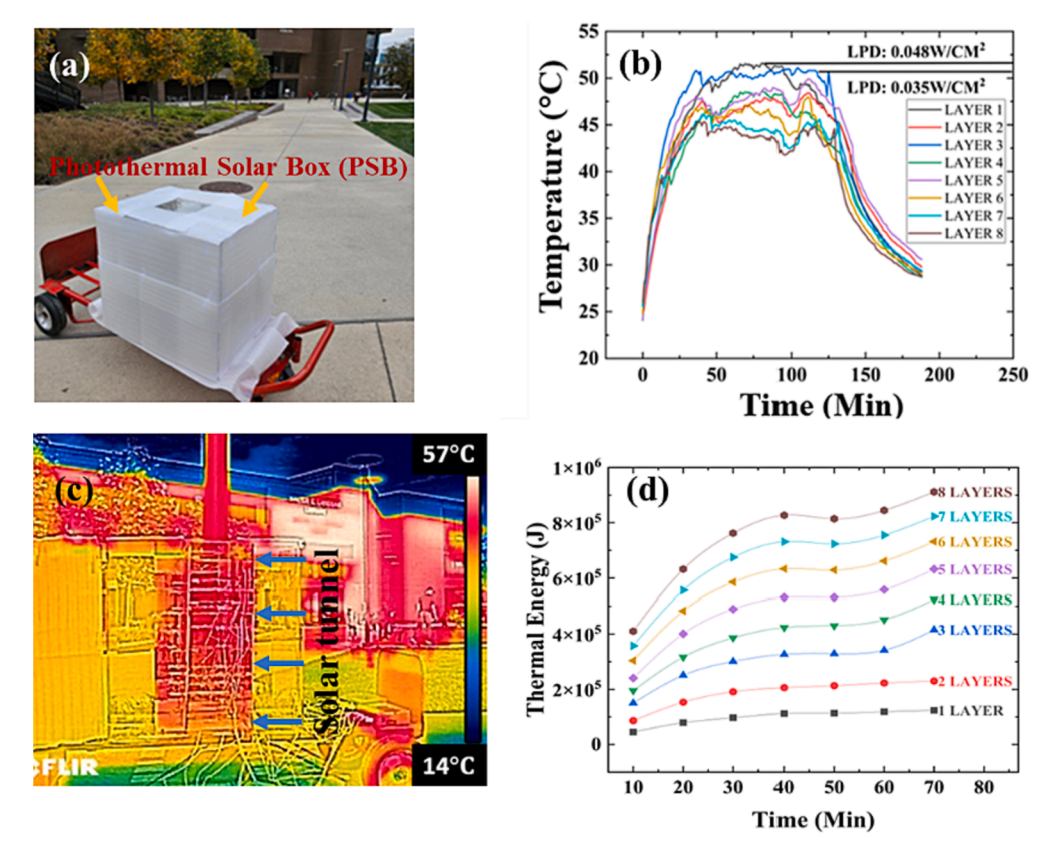


Fig. 8. (a) Schematic diagram showing the covered Photothermal Solar Box (PSB); (b) heating curves of different Transparent Photothermal Glass Panels (TPGP); (c) infrared thermal image of the PSB with 8 panels of $Fe_3O_4@Cu_{2.x}S$ films (75 % AVT) under natural sunlight entering the system from the top window; and (d) The thermal energy vs number of panels. The experiment was carried out on October 3rd, 2023, on the main campus of University of Cincinnati at 2 PM. Sunny weather. Light power density: $0.048~W/cm^2$ and $0.030~W/cm^2$. Ambient temperature: $25~^{\circ}C$.

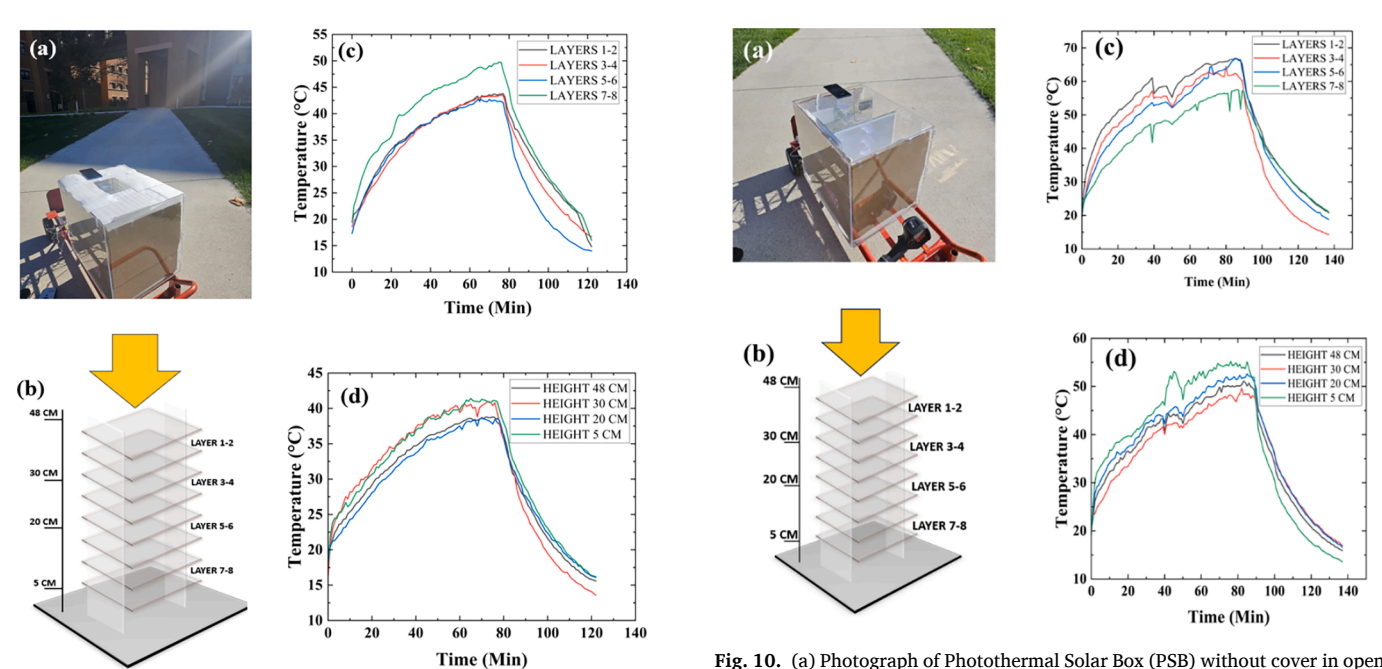


Fig. 9. (a) Photograph of Photothermal Solar Box (PSB) with cover in open air at 8 $^{\circ}$ C Ambient temperature; (b) the positions of thermometers within and outside the solar tunnel; (c) heating curves with thermometers between different TPGP as shown in (b); and (d) heating curves at different heights outside the solar tunnel as shown in (b). The experiment was carried out on November 3rd, 2023, at 2 PM. Sunny weather. Light power density: 0.048 and 0.002 W/cm². Ambient temperature: 8 $^{\circ}$ C.

Fig. 10. (a) Photograph of Photothermal Solar Box (PSB) without cover in open air at 8 $^{\circ}$ C Ambient temperature; (b) the positions of thermometers within and outside the solar tunnel; (c) heating curves with thermometers between different TPGP as shown in (b); and (d) heating curves at different heights outside the solar tunnel as shown in (b). The experiment was carried out on November 3rd, 2023, at 2 PM. Sunny weather. Light power density: 0.048 and 0.002 W/cm². Ambient temperature: 8 $^{\circ}$ C.

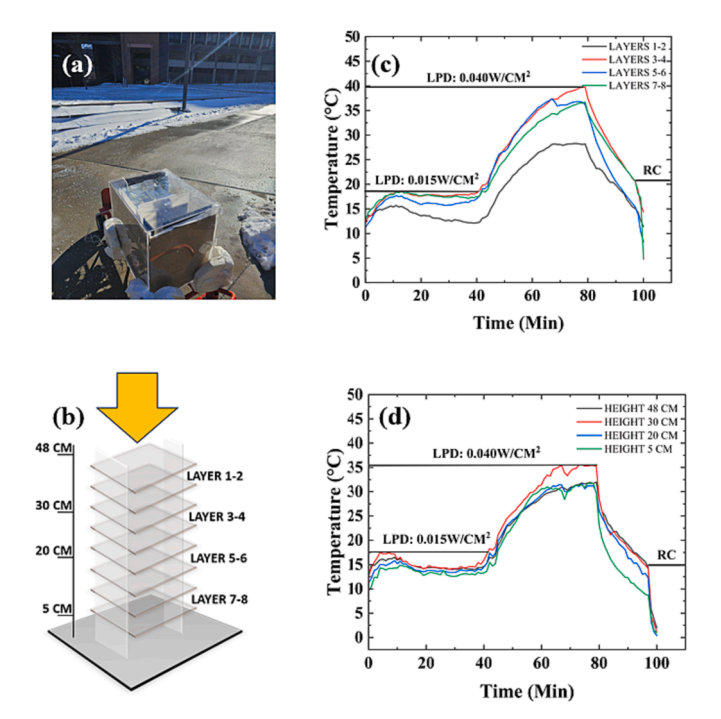


Fig. 11. (a) Photograph of Photothermal Solar Box (PSB), partially insulated, in open air at $-10~^{\circ}$ C ambient temperature; (b) the positions of thermometers within and outside the solar tunnel; (c) heating curves with thermometers between different TPGP as shown in (b); and (d) heating curves at different heights outside the solar tunnel as shown in (b). The experiment was carried out on January 20th, 2024, at 2 PM. Sunny weather. Light power density: 0.040 W/cm² and 0.002 W/cm². Ambient temperature: $-10~^{\circ}$ C.

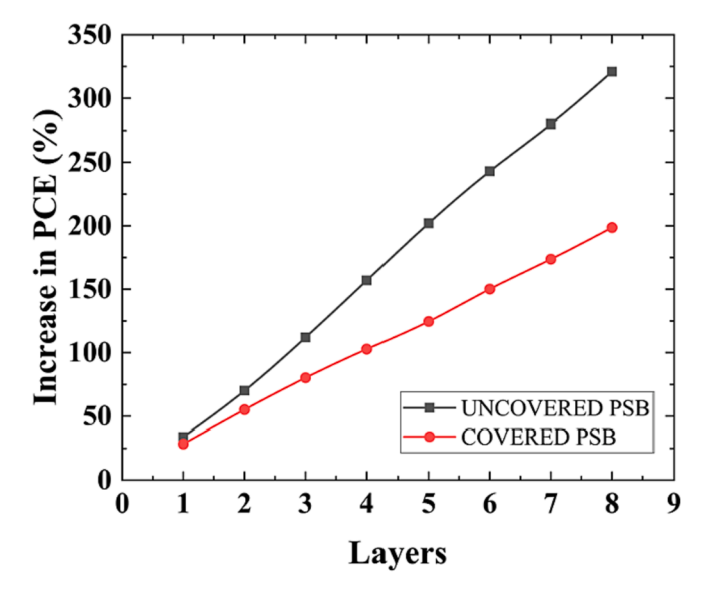


Fig. 12. Increase in Photon Conversion Efficiency (PCE) Photothermal Glass Panels (PTGP) as a function of number of TPGP. The increase in PCE is calculated using Eq. (1) for both covered and uncovered PSB.

4. Discussion

4.1. Transparency vs photothermal energy generation

The transparency of $Fe_3O_4@Cu_{2-x}S$ coated glass substrates, as depicted in Figs. 5 and 6, is a crucial factor ensuring effective photothermal energy generation in the Photothermal Solar Tunnel Radiator (PSTR). The high average visible transmittance (AVT) of 75% signifies

that these coated substrates allow light to pass through, providing a minimum of 8 TPGP (transparent panels per glass) for optimal photothermal energy absorption in the solar tunnel. The transparency of the substrates is directly linked to the unique optical absorption characteristics of the Fe₃O₄@Cu_{2-x}S compound, forming a distinctive "U"-shaped absorption profile with minimal absorption in the visible band (Fig. 5c). This absorption profile enables the penetration of sunlight through the transparent panels while efficiently activating the photothermal mechanism. However, it is essential to note that the AVT value is intricately controlled by the concentration of Fe₃O₄@Cu_{2-x}S in the thin film, introducing a contradictory relationship. While a higher concentration of Fe₃O₄@Cu_{2-x}S enhances the photothermal effect, it simultaneously reduces the AVT, impacting the transparency of the coated glass substrates. This trade-off emphasizes the need for a balanced approach in optimizing Fe₃O₄@Cu_{2-x}S concentration to achieve both efficient photothermal energy generation and satisfactory substrate transparency for the overall functionality of the PSTR system.

In pursuit of realizing the design illustrated in Fig. 2, the ideal scenario involves incorporating additional Photothermal Solar Tunnel Radiators (PSTR) to enhance the overall thermal energy generation. However, a critical consideration arises as demonstrated in Fig. 6d, where the average visible transmittance (AVT) of the multi-panel system experiences a significant drop from the initial 75% to 10% after the incorporation of 8 panels. This diminishing transparency is a consequence of the cumulative effect of multiple panels on the AVT. The challenge lies in finding a balance between increasing the number of PSTR for greater thermal energy output and maintaining satisfactory transparency in the overall system. To overcome this hurdle, it becomes imperative to focus on developing highly transparent PSTR with a robust photothermal effect through meticulous nanostructure design, precise materials synthesis, and effective property control. By strategically optimizing these factors, it is possible to engineer transparent panels that not only contribute to a more efficient solar energy harvesting system but also maintain the desired level of transparency, allowing for the successful integration of multiple PSTR units without compromising the overall performance of the system. This emphasis on transparency and photothermal efficiency underscores the importance of advancing nanoengineering approaches and material synthesis techniques for the successful implementation of scalable and high-performance solar energy harvesting systems in real-world applications.

4.2. Solar harvesting under weather conditions and photothermal energy generation

The key in this experiment is to harvest sufficient sunlight via the solar tunnel with multiple PSTR. In contrast to all conventional solar experiments with simulated light, the outdoor experiments rely on the weather and seasonal changes resulting in drastically variable light powder density. A photothermal experiment was conducted in a cloudy day on September 27th, 2023, with a covered PSB. Due to cloudy conditions, the light power density fluctuated between 0. 0001 and 0.038 $\rm W/cm^2$ resulting in two peaks in the heating curves as shown in Fig. 13. Nonetheless, the PSTR still produced considerable photothermal energy in the PSB.

Fig. 14 shows the photothermal energy absorbed and generated based on the heating curves shown in Fig. 13. The heat dynamics of transparent photothermal glass panels (TPGP) play a crucial role in the performance of the photothermal solar box (PSB). With a low specific heat capacity of TPGP (78 J/Kg.K), the panels exhibit rapid heat absorption and dissipation, as observed in Fig. 14. Under high light power density, TPGP absorbs more heat than it generates, leading to temperature elevation in both TPGP and PSB, resulting in absorption peaks. Conversely, lower light power density results in TPGP releasing excess stored heat into the PSB, resulting in generation peaks. The real-time experiment, characterized by varying light power densities, reflects the quick and dynamic interplay of heat absorption and generation,

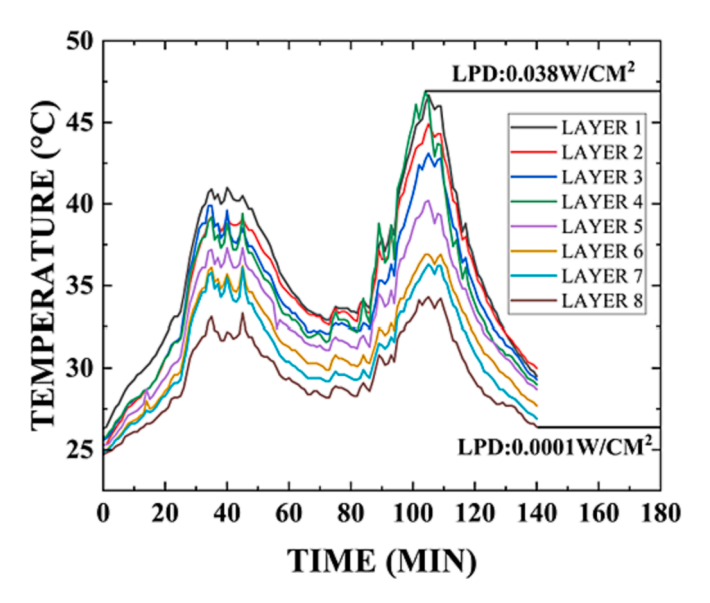


Fig. 13. Heating curves obtained in a covered PSB under cloudy weather on September 27th, 2023, on the main campus of University of Cincinnati. Ambient temperature: $25\,^{\circ}$ C. Light power density: $0.0001 - 0.038 \text{ W/cm}^2$.

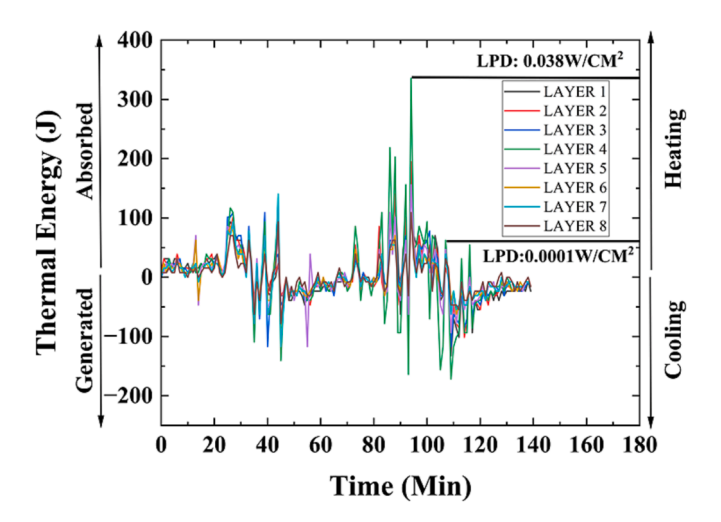


Fig. 14. The heat energy generated and absorbed by each panel over time (data draw from Fig. 13). Absorption indicates that input energy (light) surpasses output energy (heat), aligning with the heating curve. Generation denotes that input energy (light) falls short of output energy (heat), aligning with the cooling curve.

closely linked to the specific heat capacity of TPGP.

The insights derived from Fig. 14 provide a comprehensive view of the dynamic interplay between thermal energy generation and absorption over time for each Transparent Photothermal Glass Panel (TPGP). Absorption, as depicted in the graph, signifies instances where the input energy, in the form of light, exceeds the output energy, manifesting as heat. This aligns with the characteristic heating curve, where the material absorbs more energy than it dissipates. Conversely, the concept of generation comes into play when the input energy falls short of the output energy, resulting in a cooling effect. This alignment with the cooling curve illustrates phases where the material generates more heat than it absorbs. The temporal evolution of these processes, as elucidated by the graphical representation, not only provides valuable insights into the energy dynamics within each TPGP but also serves as a foundational understanding for optimizing and tailoring the performance of photothermal systems over varying operational conditions. The comprehensive analysis of these thermal dynamics contributes significantly to the

ongoing refinement and advancement of transparent photothermal technologies for diverse applications, ranging from energy-efficient building systems to solar harvesting devices.

4.3. Photothermal energy generation to maintain PSB temperature

An essential objective of this experiment is to explore the feasibility of sustaining a comfortable room temperature exclusively through solar light, as envisioned in Fig. 2. The incorporation of a white Styrofoam packing sheet in Fig. 3b serves the purpose of simulating a window structure by obstructing sunlight. As illustrated in Fig. 8b, under a warm ambient temperature of 25 °C, the Transparent Photothermal Glass Panels (TPGP) exhibit a remarkable capability to elevate their temperature to 51 °C. In colder conditions, exemplified by November in Cincinnati with an ambient temperature of 8 °C, the TPGP effectively maintain a Photothermal Solar Box (PSB) inside temperature of 40 °C (Fig. 10d), demonstrating substantial thermal energy generation. Given the appropriate thermal insulation of the PSB, it is anticipated that the internal temperature could be even higher. These experimental findings strongly suggest the practicality of harnessing solar light through the conceptual design depicted in Fig. 2, employing an array of transparent photothermal panels. Furthermore, the potential storage of thermal energy introduces the prospect of utilization during nighttime and overcast days. Building upon existing research, it is worth noting that stored thermal energy can be harnessed to generate electricity through thermoelectric generators if strategically integrated. These findings indicate the versatility and potential applications of transparent photothermal technology in achieving sustainable and energy-efficient solutions for diverse environmental conditions.

5. Summary

The conducted experiments and discussions highlight the innovative application of transparent multilayer photothermal thin films for solar harvesting, specifically in the context of building utility heating. The devised Photothermal Solar Tunnel Radiator (PSTR) demonstrates a transformative approach to energy sustainability, enabling direct solar energy harvesting through an array of transparent glass substrates with photothermal coatings. The high transparency of Fe₃O₄@Cu_{2-x}S coated glass substrates and their U-shaped optical absorption pattern contribute to efficient photothermal energy generation in the Photothermal Solar Building (PSB). Fig. 8d provides a clear representation of the thermal energy output corresponding to the number of Transparent Photothermal Glass Panels (TPGP). Remarkably, the system exhibits the ability to generate substantial thermal energy, reaching a maximum of 9.1×10^5 joules even when the Photothermal Solar Box (PSB) is covered. This noteworthy achievement is comparable to the thermal energy output of the uncovered Photothermal Solar Glass (PSG). Furthermore, Fig. 9c portrays the heating curves of the Transparent Photothermal Glass Panels (TPGP) under colder weather conditions, specifically in November with an ambient temperature of 8 °C. In contrast to the curves observed in October at a higher ambient temperature of 25 °C (Figs. 7 and 8), the temperatures now exhibit a more gradual increase, reaching their maximums at 70 min for all panels. Notably, no sustained temperature plateaus are observed due to the accelerated heat loss in the colder environment. Fig. 9d further illustrates that, despite the challenging conditions without any thermal insulations of the PSB, the interior temperatures of the Photothermal Solar Box (PSB) can achieve a commendable 40 °C at 5 cm and 30 cm depths, indicating effective photothermal heating even in cold weather. This demonstrates the robust performance and adaptability of the system to generate significant thermal energy, ensuring adequate heating within the solar box during colder periods. These findings show the resilience and efficiency of the system in harnessing solar energy, demonstrating its capacity to produce significant thermal energy under various conditions, including when the solar box is shielded.

However, the trade-off between transparency and photothermal efficiency necessitates careful consideration in achieving optimal performance. The experimental results indicate the feasibility of maintaining comfortable room temperatures solely through solar light, with the potential for thermal energy storage and utilization during periods of reduced sunlight. The innovative transparent photothermal technology offers a cost-effective and scalable alternative to traditional photovoltaic (PV) solar systems for building heating, addressing challenges such as high installation costs, space requirements, and system complexity. The experimental setup, including the transparent multilayer system and PSTR, presents a promising avenue for achieving energy-neutral building heating utilities with significant implications for sustainable and eco-friendly urban infrastructure. The findings contribute to the advancement of solar energy applications, offering a practical and efficient solution for building heating that aligns with broader goals of environmental conservation and net-zero energy consumption.

CRediT authorship contribution statement

Anudeep Katepalli: Data curation. Yuxin Wang: Data curation. Jou Lin: Data curation. Anton Harfman: Funding acquisition, Conceptualization. Mathias Bonmarin: Data curation. John Krupczak: Data curation, Supervision, Formal analysis, Methodology, Validation. Donglu Shi: Conceptulization, Funding acquisition, Writing – original draft, Writing – review & editing, Visualization, Investigationn, Validation, Formal analysis, Methodology, Supervision, Resources, Project administration.

Declaration of competing interest

The authors declare that they have no known competing financial interests or personal relationships that could have appeared to influence the work reported in this paper.

Acknowledgements

A. Katepalli et al.

We acknowledge the financial support from National Science Foundation CMMI-1953009 and the Michelman Green, Clean and Sustainable Technology Research Innovation Program (F103484).

References

- U.S. Energy Information Administration (EIA), Consumption and Efficiency, retrieved from: https://www.eia.gov/consumption/, accessed: October 2020.
- [2] F. Perera, Pollution from fossil-fuel combustion is the leading environmental threat to global pediatric health and equity: solutions exist, Int. J. Environ. Res. 15 (2018) 16
- [3] M.S. Dresselhaus, I.L. Thomas, Alternative energy technologies, Nature 414 (2001) 332–337.

- [4] M. Graetzel, Solar energy conversion by dye-sensitized photovoltaic cells, Inor. Chem. 44 (2005) 6842-6851.
- 5] R.H. Bube, Photovoltaic materials, Imperial College Press, London, UK, 1998.
- [6] V. Weitbrecht, D. Lehmann, A. Richter, Flow distribution in solar collectors with laminar flow conditions, Sol. Energy 73 (2002) 433–441.
- [7] R. Fu, D. Feldman, R. Margolis, M. Woodhouse, K. Ardani. Solar Photovoltaic System Cost Benchmark: Q1 2017. United States. U.S. Department of Energy Office of Scientific and Technical Information, DOI: 10.2172/1395932.
- [8] I. Nath, Cleaning up after clean energy: hazardous waste in the solar industry, Stanford J. Int. Relations 11 (2010) 6–15.
- [9] Irace, Phillip, Brandon, Harold, Solar heating in commercial buildings, Mech. Eng. Mater. Sci. Independent Study, 50 (2017). https://openscholarship.wustl.edu/ mems500/50.
- [10] A. Jamar, Z.A.A. Majid, W.H. Azmi, M. Norhafana, A.A. Razak, A review of water heating system for solar energy applications, Int. Commun. Heat Mass Transfer, 76 (2016) 178–187. ISSN 0735-1933, https://doi.org/10.1016/j. icheatmasstransfer.2016.05.028.
- [11] E. Monoian, R. Ferry, Return to the source, New Energy Landscapes from the Land Art Generator, Prestel, 2020.
- [12] J. Lin, M. Lyu, D. Shi, 3D solar harvesting and energy generation via multilayers of transparent porphyrin and iron oxide thin films, Energies 16 (2023) 3173, https://doi.org/10.3390/en16073173.
- [13] A. Katepalli, Y. Wang, D. Shi, Solar harvesting through multiple semi-transparent cadmium telluride solar panels for collective energy generation, Sol. Energy 264 (2023) 112047.
- [14] M. Lyu, J. Lin, D. Shi, Solar desalination via multilayers of transparent photothermal Fe3O4@Cu2–xS thin films, Energy Technology 2100590 (2021), https://doi.org/10.1002/ente.202100590.
- [15] Mengyao Lyu, Jou Lin, John Krupczak, Donglu Shi, Solar Harvesting through Multilayer Spectral Selective Iron Oxide and Porphyrin Transparent Thin Films for Photothermal Energy Generation, Adv. Sustainable Systems, https://doi.org/ 10.1002/adsu.202100006 (2021).
- [16] J. Lin, J. Krupczak, D. Shi, Solar harvesting and energy generating building skins with photothermal-photovoltaic dual modality based on porphyrin thin films, MRS Commun. (2022), https://doi.org/10.1557/s43579-022-00299-x.
- [17] J. Lin, Y. Wang, M. Lyu, D. Shi, Transparent porphyrin-based hybrid films for spectral selective solar harvesting and energy generation, Sol. Energy Mater. Sol. Cells 243 (2022) 15.
- [18] M. Lyu, J. Lin, J. Krupczak, D. Shi, Optical thermal insulation via the photothermal effects of Fe3O4 and Fe3O4@Cu2-xS thin films for energy-efficient single-pane windows, MRS Commun. 10 (3) (2020) 439–448.
- [19] M.E. Sadat, M.K. Baghbador, A.W. Dunn, H.P. Wagner, R.C. Ewing, J. Zhang, X. u. Hong, G.M. Pauletti, D.B. Mast, Donglu Shi, Photoluminescence and photothermal effect of Fe3O4 nanoparticles for medical imaging and therapy, Appl. Phys. Lett. 105 (9) (2014) 091903.
- [20] J. Lin, Y. Zhao, D. Shi, Light angle dependence of photothermal properties in oxide and porphyrin thin films for energy-efficient window applications, MRS Commun. 10 (2020) 155–163.
- [21] Donglu Shi, M.E. Sadat, A.W. Dunn, David B. Mast, Photo-fluorescent and magnetic properties of iron oxide nanoparticles for biomedical applications, Nanoscale 7 (18) (2015) 8209–8232.
- [22] Y. Jou Lin, D.S. Zhao, Optical thermal insulation via the photothermal effects of Fe3O4 and Fe3O4@Cu2-xS thin films for energy-efficient single-pane windows, MRS Commun. 10, 1 (2020) 155–163, https://doi.org/10.1557/mrc.2020.4.
- [23] J. Lin, J. Krupczak, D. Shi, Solar harvesting and energy generating building skins with photothermal-photovoltaic modality based on porphyrin thin films, MRS Commun. (2022), https://doi.org/10.1557/s43579-022-00299-x.
- [24] J. Lin, D. Shi, Photothermal and photovoltaic properties of transparent thin films of porphyrin compounds for energy applications, Appl. Phys. Rev. 8 (2021) 011302, https://doi.org/10.1063/5.0036961.